©2026 Ada Academica https://adac.ee

Eur. J. Math. Anal. 6 (2026) 12
doi: 10.28924/ada/ma.6.12

Mathematical Analysis of Corruption Dynamics Incorporating the Corrupt Individuals Under Investigation Class and Recidivism

Francis Musili Muli

Department of Mathematics Sciences, The Co-operative University of Kenya, Nairobi, Kenya
Correspondence: framuli2011@gmail.com

Abstract. Corruption is a complicated social, political, and economic phenomenon that impacts both public and private officials, as well as the nation as a whole. Several studies have likened it to an harrowing contagious disease because of its propensity to proliferate in the society by replicating itself from one individual to another and it causes debilitating effects to a country's economy. Despite the fact that many nations employ a variety of strategies to curb the spread of corruption, the vice incessantly persists. To ascertain the impact of control measures on corruption's propagation, a nonlinear deterministic mathematical model that describes its dynamics is developed and analyzed in this study. The study incorporates rigorous analysis to verify the existence, positivity, and boundedness of the solution, as well as the stability of the equilibrium points. It is confirmed that whenever the corruption reproduction number R_0 is less than one, the corruption-free equilibrium (CFE) is globally asymptotically stable. Using the normalized forward sensitivity approach, we determined the prerequisite for the optimal approach to mitigate the propagation of corruption. It is evident that 10% increase in corruption initiation rate β causes a corresponding 10% increase in R_0, while 10% increase in efficacy of anti-corruption and religious instructions ψ as well as incarceration rate γ_3 causes a reduction of R_0 by 6.462% and 1.686% respectively. On the numerical segment, python software was utilized to illustrate the time series solution. The numerical findings were in concurrence with the analytical results. This study recommends a tripartite approach to eradicating corruption over time. This involves effective anti-graft campaigns and religious teaching, establishment of an efficient and robust whistle-blowing protocols and lastly the imprisonment of individuals found culpable of committing corruption regardless of their socio-economic statuses.

1. Introduction

With a large population living in extreme poverty, Sub-Saharan Africa is typically regarded as the world's poorest region. Coincidentally, it is arguably regarded as the home of some of the most corrupt and ethnically divided nations on earth. Consequently, a number of studies have correlated corruption and subpar governance with the number of ethnic fragmentation, arguing that the more tribes a nation has, the more impoverished and corrupt it is [1, 2]. The

Received: 25 Jun 2026.
Key words and phrases. Corruption; Recidivism; Suspects; Stability analysis; Forward bifurcation; Numerical analysis.

study by [3] gave an account of postcolonial Africa's corruption. The study finding revealed that patronage-based political and cultural practices are the root cause of widespread corruption in African countries, often made worse by a strong sense of entitlement. This makes the concept of African remedies to African problems practically a difficult and daunting task. According to [4–6], corruption immensely impedes economic growth by lowering foreign direct and domestic investments, aggrandizing government expenditure, and redirecting funds meant for infrastructure maintenance, health care, and education to less prioritized public projects that are more vulnerable to bribery and manipulation. According to the World Bank, corrupt practices are the biggest barriers to social and economic growth because they sabotage the rule of law and the institutional underpinnings that support economic prosperity. Furthermore, they jeopardize international reputation, peace and national security [7]. It is indisputable that mathematical modeling has played a crucial role of not only helping to comprehend the dynamics of corruption propagation but also influencing intervention strategies. The study conducted by [8] used a corruption model that included five compartments: susceptible (S), exposed (E), corrupt (C), incarcerated (J), and honest (H). According to the study, the best ways to stop corruption from spreading were to lower the effective transmission contact rate and implement a suitable penalty rate. Adetayo et al. [9] proposed a mathematical model to study the impact of corruption in a society where honest individuals are prone to become corrupt. The analytical and numerical analysis of the study suggested that the factors that have the greatest impact on corruption dynamics are the rate at which corrupt people are imprisoned, the frequency with which exposed people turn corrupt, and the contact rate between corrupt and honest people. The study conducted by [10] looked at how religion, education, and punishment affected the dynamics of corruption transmission, as well as the potential for honest people to revert to the susceptible class. According to the research findings, religious leaders must play a crucial role in teaching the congregants about the detrimental effects of corruption. A mathematical model with a constant recruitment rate was developed and examined by Lemecha [11]. The model considered the awareness brought about by inmate counseling and anti-corruption programs. The study found that the corruption-free equilibrium is locally asymptotically stable whenever the reproduction number is smaller than one. Numerical simulation was used to validate the analytical results.

The corrupt individuals under investigation compartment, has been disregarded by numerous models. Exposure and reporting of corruption can result in public scrutiny, legal action, and investigations, all of which can be instrumental in abating the frequency of corrupt activities. The possibility that honest people could turn corrupt after interacting with corrupt people has also been taken into account. This study also examines the prospects of recidivism; the occurrence where people revert to corrupt practices after being cautioned by the court against doing so.

The organization of this article is as follows: Sec.2 gives the in-depth examination of the model's characteristics, including stability, bifurcation analysis, invariant region, reproduction number, positivity, and boundedness, is covered in Section. In Sec.3 the key findings from numerical simulations are investigated, along with sensitivity analysis, and results are displayed using Python software. The conclusions part is presented in Sec.4.

1.1. **Model formulation.** To better understand the dynamics of corruption, a mathematical model has been developed that an extension of the research conducted in [10] including (i) the suspect class (I), which comprises individuals under investigation for corruption-related crimes, and (ii) the jail class (J), comprising individuals indicted and incarcerated for corruption-related offenses. The entire population is thus partitioned into seven non-overlapping compartments comprising the susceptible (S), honest (H), exposed population (E), corrupt (C), corrupt individuals under investigation (I), imprisoned (J), and recovered (R) individuals.

The rate at which individuals enter the susceptible population is Λ. All persons are predisposed to be susceptible to corruption by birth. A proportion of susceptible individuals become honest at the rate θ as a result of anti-graft campaigns and religious teachings. A modification factor ψ $(0 < \psi < 1)$ accounts for the reduced contact rate of corrupted individuals with honest individuals relative to susceptible individuals. Individuals transition from vulnerable and truthful states to corrupt states following successful encounters with corrupt individuals. This study adopts a standard incidence force of initiation into corrupt practices and is expressed as

$$\lambda_c(t) = \frac{\beta(C(t) + \omega I(t))}{N - J}$$

excluding the imprisoned individuals, which is synonymous with that of infectious diseases and drug abuse models as utilized in [12–14]. The parameter ω $(0 < \omega < 1)$ accounts for the reduced infectiousness of the suspect individuals relative to those in a corrupt state. The interaction of the susceptible and the honest individuals with corrupt individuals leads to the growth of the exposed class at rates λ and $(1 - \psi)\lambda$. Individuals exit corrupt compartment at the rate α in which a proportion τ recover while $(1 - \tau)$ become corrupt. People who actively participate in corrupt activities make up the corrupt state $C(t)$. Individuals exit this compartment as a result of anti-corruption sensitization and religious teachings at the rate η_2 while others join the suspect class at the rate η_1. People in the suspect class I are being investigated for alleged corruption. A proportion γ_1 of people exit this class and relapse into corrupt behavior while γ_3 of the individuals are incarcerated for being culprits of corrupt malpractices. The parameter σ is the average period of time a prisoner spends in Jail. Finally, the recovered compartment is increased at rate τ, η_2, γ_2 and σ as a result of cessation of corrupt practices by the exposed, corrupt, suspect and jailed individuals respectively. The number of people in each compartment is decreased by μ, which accounts for natural death rate. Table (1) and Table (2) give the summary of state variables and the parameter values respectively. Consequently, the proposed model's system of non-linear differential equations is as follows:

$$\begin{aligned}
\frac{dS}{dt} &= \Lambda + \rho H + \zeta R - \frac{\beta(C(t)+\omega I(t))S}{N-J} - (\mu+\theta)S,\\
\frac{dH}{dt} &= \theta S - \frac{(1-\psi)\beta(C(t)+\omega I(t))H}{N-J} - (\mu+\rho)H,\\
\frac{dE}{dt} &= \frac{\beta(C(t)+\omega I(t))S}{N-J} + \frac{(1-\psi)\beta(C(t)+\omega I(t))H}{N-J} - (\mu+\alpha)E,\\
\frac{dC}{dt} &= \alpha(1-\tau)E + \gamma_1 I - (\mu+\eta_1+\eta_2)C,\\
\frac{dI}{dt} &= \eta_1 C - (\mu+\gamma_1+\gamma_2+\gamma_2)I,\\
\frac{dJ}{dt} &= \gamma_3 I - (\mu+\sigma)J,\\
\frac{dR}{dt} &= \alpha\tau E + \eta_2 C + \gamma_2 I + \sigma J - (\mu+\zeta)R,
\end{aligned} \tag{1}$$

where the initial conditions are: $S(0) = S_0 \geq 0, H(0) = H_0 \geq 0, E(0) = E_0 \geq 0, C(0) = C_0 \geq 0, I(0) = I_0 \geq 0, J(0) = J_0 \geq 0, R(0) = R_0 \geq 0$.

To ease the mathematical operation of the system (1) of the differential equations, we adopt the following notations: $\kappa_0 = (\mu+\rho+\theta)$, $\kappa_1 = (\mu+\theta)$, $\kappa_2 = (\mu+\rho)$, $\kappa_3 = (\mu+\alpha)$, $\kappa_4 = (\mu+\eta_1+\eta_2)$, $\kappa_5 = (\mu+\gamma_1+\gamma_2+\gamma_3)$, $\kappa_6 = (\mu+\sigma)$ and $\kappa_7 = (\mu+\zeta)$

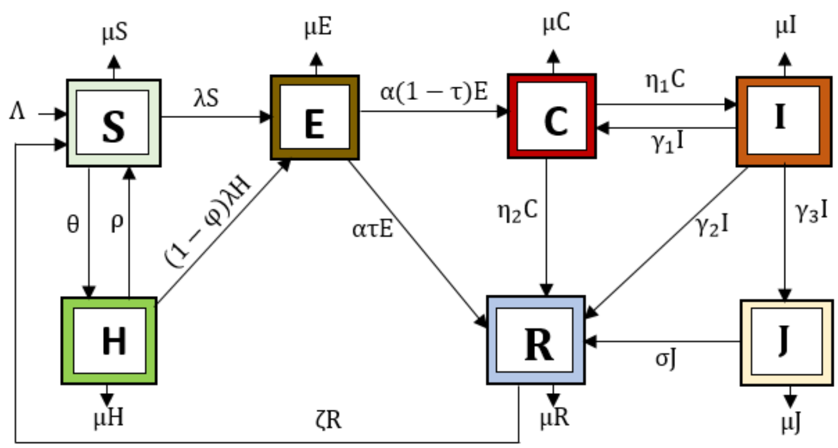

Figure 1. Diagrammatic representation of corruption dynamics model (1).

2. Model Analysis

This section examines the fundamental characteristics of the suggested model, including the bifurcation analysis, the solution's positivity and boundedness, the local and global analysis of drug-free and drug abuse-endemic equilibria.

Table 1. Definition of state variables

Variable	Definition
S	Individuals susceptible to corruption
H	Honest Population
E	Corrupt-related exposed population
C	The corrupt population
I	Corrupt population under investigation
J	The jailed population
R	The populace recovered from corrupt acts

Table 2. Definition of model parameters

Variable	Definition
Λ	Rate at which a susceptible cohort is recruited from the general population
β	The corruption initiation rate
ρ	Rate of honest individuals becoming susceptible
ψ	Efficacy of religious and anti-corruption campaign
θ	Rate of change of susceptible due to religious and anti-corruption campaign
μ	Natural mortality rate
τ	The proportion of the exposed persons who get join recovered compartment
γ_1	Rate of recidivism of corrupt individuals under investigation
γ_2	Rate at corrupt individuals under investigation quit corrupt practices
γ_3	Rate of conviction and incarceration of persons under investigation
α	The rate of at which individuals exit the exposed compartment
ζ	Rate at which recovered individuals become susceptible
ω	The modification coefficient of corrupt individuals under investigation
σ	Average period of time prisoners spent in jail
η_1	Rate at which corrupt individuals are identified
η_2	Rate of recovery of corrupt individuals

2.1. **Positivity and boundedness.** To confirm the model's validity, we must first demonstrate that the model equations' solutions (1) are positive. A theorem and it's proof are utilized to illustrate this truth.

Theorem 1. *If $S(0), H(0), C(0), I(0), J(0)$ and $R(0)$ are all greater than or equal to zero, then it is apparent that the solutions $S(t), H(t), C(t), I(t), J(t)$ and $R(t)$ of model (1) are positive for all $t > 0$.*

Proof. It is evident that $S(t) > 0$, for all $t \geq 0$. If not, let there exist $t_i > 0$ such that $S(t_i) = 0$ and $S^{'}(t_i) \leq 0$ for all $0 \leq t \leq t_i$. Then, utilizing equation one of the model(1) gives

$$\frac{d}{dt}\left(S(t)e^{(\lambda+\kappa_1)t}\right) = \Lambda e^{(\lambda+\kappa_1)t}. \tag{2}$$

Integrating equation (2) from 0 to t_i gives:

$$S(t_i)e^{(\lambda+\kappa_1)t_i} - S(0) = \int_0^{t_i} \Lambda e^{(\lambda+\kappa_1)\nu} d\nu. \tag{3}$$

Multiplying each term of equation (3) by $e^{-(\lambda(t_i)+\kappa_1)t_i}$ yields,

$$S(t_i) = \left\{ S(0)e^{-(\lambda+\kappa_1)t_i} + e^{-(\lambda+\kappa_1)t_i} \left[\int_0^{t_i} \Lambda e^{(\lambda+\kappa_1)\nu} d\nu \right] \right\} > 0. \tag{4}$$

This is a contradiction since $S(t_i) = 0$. The implication of this is that $S(t) > 0$ for all $t > 0$. In a similar manner, it can be shown that $H(t) = E(t) = C(t) = I(t) = J(t) = R(t) > 0 \ \forall t > 0$. This concludes the proof of the positivity of the model state variables. □

Theorem 2. *The solution set* $\{S(t), H(t), E(t), C(t), I(t), J(t), R(t)\}$ *of model system (1) is bounded in a feasible region* Ω.

Proof. Consider the feasible region $\Omega = \{S(t), H(t), E(t), C(t), I(t), J(t), R(t)\} \in \mathbb{R}^7_+$. Then for the total population, we have, $\frac{dN}{dt} = \Lambda - \mu N$. Using the method of separation of variables and considering the initial condition, it can be shown that $N(t) = \frac{\Lambda}{\mu} + \{\frac{\Lambda}{\mu} - N(0)\}e^{-\mu t}$. We note that $N_{t\to\infty} = \frac{\Lambda}{\mu}$. Since $e^y \geq 0, \forall y$, it is evident that $N(t) \leq \frac{\Lambda}{\mu}$. This demonstrates that the soluton of the model system (1) is bounded and Ω is an invariant region. The biological interpretation of the model solution's boundedness suggests that biological processes are inherently limited or that population growth is constrained by nature. □

2.2. **Corruption-free equilibrium.** In a community devoid of corruption, where $E = C = I = J = R = 0$, the corruption-free equilibrium (CFE), denoted by ε_0, is stable. Equating the first two equation in the model equation (1) to zero and evaluating gives, $S^0 = \frac{\Lambda(\mu+\rho)}{\mu(\mu+\rho+\theta)}$ and $H^0 = \frac{\Lambda\theta}{\mu(\mu+\rho+\theta)}$. Thus, the CFE state is provided as,

$$\varepsilon_0 = \{S^0, H^0, E^0, C^0, I^0, J^0, R^0\} = \left\{ \frac{\Lambda(\mu+\rho)}{\mu(\mu+\rho+\theta)}, \frac{\Lambda\theta}{\mu(\mu+\rho+\theta)}, 0, 0, 0, 0, 0 \right\}. \tag{5}$$

We note that the total population at corruption-free equilibrium is given by

$$N = S^0 + H^0 = \frac{\Lambda(\mu+\rho)}{\mu(\mu+\rho+\theta)} + \frac{\Lambda\theta}{\mu(\mu+\rho+\theta)} = \frac{\Lambda}{\mu}.$$

.

2.3. **The basic reproduction number.** A key parameter in epidemiology is the basic reproduction number R_0, which is commonly defined as the average number of secondary cases that an infectious individual causes in a community that is completely susceptible [15,16]. In addition to deriving this parameter, our analysis looks at how sensitive it is to different influences, which can help guide specific management methods. Using Lyapunov functions, we further examine both local and global stability, illustrating the circumstances in which corruption either disappears or continues to exist in the populace. To determine the basic reproduction number of our model in (1), we employ the Next-generation matrix approach presented by the authors in [16]. Considering the corruption infected compartments, the transition and transmission matrices, denoted by $\mathcal{F}$ and $\mathcal{V}$ respectively are given by:

$$\mathcal{F} = \begin{pmatrix} 0 & \frac{\beta(\theta(1-\psi)+\mu+\rho)}{(\mu+\rho+\theta)} & \frac{\beta\omega(\theta(1-\psi)+\mu+\rho)}{(\mu+\rho+\theta)} & 0 \\ 0 & 0 & 0 & 0 \\ 0 & 0 & 0 & 0 \\ 0 & 0 & 0 & 0 \end{pmatrix},$$

and

$$\mathcal{V} = \begin{pmatrix} \kappa_3 & 0 & 0 & 0 \\ -\alpha\tau_1 & \kappa_4 & -\gamma_1 & 0 \\ 0 & \eta_1 & \kappa_5 & 0 \\ 0 & 0 & -\gamma_3 & \kappa_6 \end{pmatrix}.$$

The basic reproduction number is considered as the largest eigenvalue of the next generation matrix $\mathcal{F}\mathcal{V}^{-1}$. Simple computations allow us to demonstrate that:

$$\mathcal{V}^{-1} = \begin{pmatrix} \frac{1}{\kappa_3} & 0 & 0 & 0 \\ \frac{\alpha\kappa_5\tau_1}{\kappa_3(\kappa_4\kappa_5-\eta_1\gamma_1)} & \frac{\kappa_5}{\kappa_4\kappa_5-\eta_1\gamma_1} & \frac{\kappa_4}{\kappa_4\kappa_5-\eta_1\gamma_1} & 0 \\ \frac{\alpha\eta_1\tau_1}{\kappa_3(\kappa_4\kappa_5-\eta_1\gamma_1)} & \frac{\eta_1}{\kappa_4\kappa_5-\eta_1\gamma_1} & \frac{\kappa_4}{\kappa_4\kappa_5-\eta_1\gamma_1} & 0 \\ \frac{\alpha\eta_1\gamma_3\tau_1}{\kappa_3\kappa_6(\kappa_4\kappa_5-\eta_1\gamma_1)} & \frac{\eta_1\gamma_3}{\kappa_6(\kappa_4\kappa_5-\eta_1\gamma_1)} & \frac{\gamma_3\kappa_4}{\kappa_6(\kappa_4\kappa_5-\eta_1\gamma_1)} & \frac{1}{\kappa_6} \end{pmatrix},$$

where we define the notation utilized as: $\kappa_3 = (\mu+\alpha)$, $\kappa_4 = (\mu+\eta_1+\eta_2)$, $\kappa_5 = (\mu+\gamma_1+\gamma_2+\gamma_3)$, and $\kappa_6 = (\mu+\sigma)$. The next generation matrix is ascertained as follows:

$$\mathcal{F}\mathcal{V}^{-1} = \begin{pmatrix} \frac{\alpha\beta\tau_1(\theta\psi_1+\kappa_2)(\omega\eta_1+\kappa_5)}{\kappa_0\kappa_3(\kappa_4\kappa_5-\eta_1\gamma_1)} & \frac{\beta(\theta\psi_1+\kappa_2)(\omega\eta_1+\kappa_5)}{\kappa_0(\kappa_4\kappa_5-\eta_1\gamma_1)} & \frac{\beta(\theta\psi_1+\kappa_2)(\gamma+\omega\kappa_4)}{\kappa_0(\kappa_4\kappa_5-\eta_1\gamma_1)} & 0 \\ 0 & 0 & 0 & 0 \\ 0 & 0 & 0 & 0 \\ 0 & 0 & 0 & 0 \end{pmatrix}.$$

The basic reproduction number R_0 for the corruption model can be obtained from the most prominent eigenvalue of the next generation matrix, $\mathcal{F}\mathcal{V}^{-1}$ as defined in [15].

$$\mathrm{R}_0 = \frac{\alpha\beta(1-\tau)(\theta(1-\psi)+\mu+\rho)(\omega\eta_1+\mu+\gamma_1+\gamma_2+\gamma_3)\}}{(\mu+\theta+\rho)(\mu+\alpha)((\mu+\eta_1+\eta_2)(\mu+\gamma_2+\gamma_3)+\gamma_1(\mu+\eta_2))}. \tag{6}$$

where $\alpha_1 = (\mu+\psi)$. We also let $(\mu+\xi) = \Phi$, $\alpha_6 = (\alpha_4\alpha_5-\rho\tau) = \{\tau(\zeta+\delta_2+\vartheta+\mu)+\alpha_5(\delta_1+\mu)\} > 0$ and $\alpha_8 = (\alpha_3\alpha_5-\eta_2\vartheta) = \{(\mu+\eta_1+\eta_3)(\mu+\rho+\zeta+\vartheta+\delta_2)+\eta_2(\mu+\rho+\zeta+\delta_2)\} > 0$.

2.4. **The Local stability of corruption-free equilibrium (CFE).**

Theorem 3. *For the model (1), the CFE point (ε_0) is locally asymptotically stable when $R_0 < 1$ and unstable whenever $R_0 > 1$.*

Proof. We determine the Jacobian of the system (1) at CFE to give

$$J_{\varepsilon_0} = \begin{pmatrix} -\kappa_1 & \rho & 0 & -\frac{\beta(\mu+\rho)}{\mu+\rho+\theta} & -\frac{\beta\omega(\mu+\rho)}{\mu+\rho+\theta} & 0 & \zeta \\ \theta & -\kappa_2 & 0 & -\frac{\beta\theta(1-\psi)}{\mu+\rho+\theta} & -\frac{\beta\theta\omega(1-\psi)}{\mu+\rho+\theta} & 0 & 0 \\ 0 & 0 & -\kappa_3 & \frac{\beta(\theta(1-\psi)+\mu+\rho)}{\mu+\rho+\theta} & \frac{\beta\omega(\theta(1-\psi)+\mu+\rho)}{\mu+\rho+\theta} & 0 & 0 \\ 0 & 0 & \alpha(1-\tau) & -\kappa_4 & \gamma_1 & 0 & 0 \\ 0 & 0 & 0 & \eta_1 & -\kappa_5 & 0 & 0 \\ 0 & 0 & 0 & 0 & \gamma_3 & -\kappa_6 & 0 \\ 0 & 0 & \alpha\tau & \eta_2 & \gamma_2 & \delta & -\kappa_7 \end{pmatrix}. \tag{7}$$

The first, second, sixth and the seventh eigenvalues are $-(\mu+\rho+\theta) < 0, -\mu < 0, -(\mu+\rho) < 0$ and $-(\mu+\zeta) < 0$ respectively. These eigenvalues are clearly identifiable from the Jacobian matrix J_{ε_0}. The remaining eigenvalues can be evaluated by using the reduced matrix (8).

$$J|_{\varepsilon_{0R}} = \begin{pmatrix} -(\mu+\alpha) & \frac{\beta(\theta(1-\psi)+\mu+\rho)}{\mu+\rho+\theta} & \frac{\beta\omega(\theta(1-\psi)+\mu+\rho)}{\mu+\rho+\theta} \\ \alpha(1-\tau) & -(\mu+\eta_1+\eta_2) & \gamma_1 \\ 0 & \eta_1 & -(\mu+\gamma_1+\gamma_2+\gamma_3) \end{pmatrix}. \tag{8}$$

From $|J|_{\varepsilon_{0R}} - \lambda\mathbf{I}| = 0$, we are able to determine the characteristic equation, where $\mathbf{I}$ is a three-by-three identity matrix. This gives

$$\lambda^3 + \mathcal{Q}_2\lambda^2 + \mathcal{Q}_1\lambda + \mathcal{Q}_0 = 0, \tag{9}$$

where $\mathcal{Q}_2 = \kappa_3 + \kappa_4 + \kappa_5$, $\mathcal{Q}_1 = \frac{\kappa_3(\kappa_4\kappa_5-\eta_1\gamma_1)}{\kappa_5+\eta_1\omega}(\mathcal{M} - \mathrm{R}_0)$, $\mathcal{Q}_0 = \kappa_3(\kappa_4\kappa_5 - \eta_1\gamma_1)(1 - \mathrm{R}_0)$ and $\mathcal{M} = \frac{(\kappa_3(\kappa_4+\kappa_5)+\kappa_4\kappa_5-\eta_1\gamma_1)(\eta_1\omega+\kappa_5)}{\kappa_3(\kappa_4\kappa_5-\eta_1\gamma_1)}$

We now utilize Routh-Hurwitz criteria [17, 18], which states that the necessary and sufficient conditions for all the solutions of the characteristic equation (9) to possess a negative real is that $\mathcal{Q}_j > 0$ and

$\mathcal{P}_1 = \mathcal{Q}_1 > 0$, $\mathcal{P}_2 = \begin{vmatrix} \mathcal{Q}_2 & 1 \\ \mathcal{Q}_0 & \mathcal{Q}_1 \end{vmatrix} > 0$. It is evident that $\mathcal{P}_1 > 0$. Moreover, $\mathcal{P}_3 > 0$ whenever $\mathrm{R}_0 < 1$. We also note that $\mathcal{M} > 1$ which implies that $\mathcal{Q}_0$ is also positive whenever $\mathrm{R}_0 < 1$. It is therefore imperative that by the Routh-Hurwitz criteria, the CFEP (ε_0) is locally asymptotically stable whenever $\mathrm{R}_0 < 1$ and $\mathcal{Q}_1\mathcal{Q}_2 > \mathcal{Q}_0$. □

The local stability of ε_0 when $\mathrm{R}_0 < 1$ suggests that, following small perturbations, the system will revert to its corruption-free equilibrium. In a biological sense, this indicates that the average corrupt person spreads their corrupt behavior to fewer than one other person, suggesting that the initiation rate is too low for corruption to spread or endure across the community.

2.5. **Global Stability of CFE.** For the global stability of CFE, we utilize the approach of Castillo-Chavez and Song [19]. To do this, we first split the model (1) into two subsystems of corruption free vector $\mathbb{F}(\Gamma_1, \Gamma_2)$ and corruption-infected vector $\mathbb{G}(\Gamma_1, \Gamma_2)$ as:

$$\begin{cases} \frac{d\Gamma_1}{dt} = \mathbb{F}(\Gamma_1, \Gamma_2), \\ \frac{d\Gamma_2}{dt} = \mathbb{G}(\Gamma_1, \Gamma_2), \ \mathbb{G}(\Gamma_1, 0) = 0, \end{cases} \tag{10}$$

where $\Gamma_1 = (S, H, R) \in \mathbb{R}^3$ and $\Gamma_2 = (E, C, I, J) \in \mathbb{R}^4_+$. For the system to exhibit global asymptomatic stability at corruption-free equilibrium, the following constraints must be met.

(i) $\frac{d\Gamma_1}{dt} = \mathbb{F}(\Gamma_1, 0), \Gamma_1^0 = (S^0, H^0, R^0)$ is globally asymptotically stable.

(ii) $\frac{d\Gamma_2}{dt} = \frac{dG}{d\Gamma_2}|_{(\Gamma_1,0)}\Gamma_2 - \tilde{\mathbb{G}}(\Gamma_1, \Gamma_2), \implies \tilde{\mathbb{G}}(\Gamma_1, \Gamma_2) \geq 0$, where $\frac{dG}{d\Gamma_2}|_{(\Gamma_1,0)}$ is an M-matrix.

Theorem 4. *For the model (1), the corruption-free equilibrium point ε_0 is globally asymptotically stable provided that $\mathrm{R}_0 < 1$ and that the criteria (i) and (ii) are met.*

Proof. First, we verify condition (i) by taking into consideration that

$$\mathbb{F}(\Gamma_1, 0) = \begin{pmatrix} \Lambda + \rho H + \zeta R - \kappa_1 S \\ \theta S - \kappa_2 H \\ -\kappa_7 R \end{pmatrix}. \tag{11}$$

Making use of equation (11) it can be demonstrated that as time t tends to infinity, all states approach corruption-free equilibrium point. We now consider the second condition:

$$\mathbb{G}(\Gamma_1, \Gamma_2) = \begin{pmatrix} \lambda S + (1-\psi)\lambda H - \kappa_3 E \\ \alpha(1-\tau)E + \gamma_1 I - \kappa_4 C \\ \eta_1 C - \kappa_5 I \\ \gamma_3 I - \kappa_6 J \end{pmatrix}. \tag{12}$$

We find the partial derivative of equation (12) with respect to Γ_2 computed at $(\Gamma_1, 0)$ to get,

$$\frac{dG}{d\Gamma_2}|_{(\Gamma_1,0)} = \begin{pmatrix} -\kappa_3 & \frac{\beta\{S^o+(1-\psi)H^0\}}{N^o} & \frac{\omega\beta\{S^o+(1-\psi)H^0\}}{N^o} & 0 \\ \alpha(1-\tau) & -\kappa_4 & \gamma_1 & 0 \\ 0 & \eta_1 & -\kappa_5 & 0 \\ 0 & 0 & \gamma_3 & -\kappa_6 \end{pmatrix}, \tag{13}$$

where $N^0 = S^0 + H^0$.

Since every element on the main diagonal is negative and every other entry is positive, this makes $\frac{dG}{d\Gamma_2}|_{(\Gamma_1,0)}$ an M-matrix [20]. We now proof the condition $\tilde{\mathbb{G}}(\Gamma_1, \Gamma_2) \geq 0$. We consider,

$$\frac{dG}{d\Gamma_2}|_{(\Gamma_1,0)}\Gamma_2 = \begin{pmatrix} -\kappa_3 E + \frac{\beta\{S^o+(1-\psi)H^0\}C}{N^o} + \frac{\omega\beta\{S^o+(1-\psi)H^0\}I}{N^o} \\ \alpha(1-\tau)E - \kappa_4 C + \gamma_1 I \\ \eta_1 C - \kappa_5 I \\ \gamma_3 I - \kappa_6 J \end{pmatrix}, \tag{14}$$

Since $\tilde{\mathbb{G}}(\Gamma_1,\Gamma_2) = \frac{dG}{d\Gamma_2}|_{(\Gamma_1,0)}\Gamma_2 - \mathbb{G}(\Gamma_1,\Gamma_2)$, we carry out some algebraic manipulation to obtain,

$$\tilde{G}(\Gamma_1,\Gamma_2) = \begin{pmatrix} \frac{\lambda S^0 N_J}{N0}\left(1-\frac{SN^0}{S^0N_J}\right) + \frac{\lambda(1-\psi)H^0N_J}{N^0}\left(1-\frac{HN^0}{H^0N_J}\right) \\ 0 \\ 0 \\ 0 \end{pmatrix}, \tag{15}$$

where $N_J = N - J$.

In equation (15), we can observe that for any $(\Gamma_1,\Gamma_2) \in \Omega$, $\tilde{\mathbb{G}}(\Gamma_1,\Gamma_2) \geq 0$. This implies that corruption-free equilibrium is globally asymptotically stable as long as $R_0 < 1$ since both criteria(i) and (ii) are satisfied. □

The findings of theorem (3) explicitly show that the system will tend towards ε_0 irrespective of the values of the initial state variables.

2.6. **Existence of corruption endemic equilibrium.** The endemic equilibrium in our model is driven by persistent corruption in the community. For this equilibrium, we use $\varepsilon^* = (S^*, H^*, E^*, C^*, I^*, J^*, R^*)$. We denote the force of initiation into corrupt habits by

$$\lambda^* = \frac{\beta(C^* + \omega H^*)}{N^* - J^*}. \tag{16}$$

To obtain the value of ε^*, we set model (1) to zero i.e.

$$\begin{aligned}
0 &= \Lambda + \rho H^* + \zeta R^* - \lambda^* S^* - (\mu+\theta)S^*,\\
0 &= \theta S^* - (1-\psi)H^*\lambda^* - (\mu+\rho)H^*,\\
0 &= \lambda^* S^* + (1-\psi)H^*\lambda^* - (\mu+\alpha)E^*,\\
0 &= \alpha(1-\tau)E^* + \gamma_1 I^* - (\mu+\eta_1+\eta_2)C^*,\\
0 &= \eta_1 C^* - (\mu+\gamma_1+\gamma_2+\gamma_3)I^*,\\
0 &= \gamma_3 I^* - (\mu+\sigma)J^*,\\
0 &= \alpha\tau E^* + \eta_2 C^* + \gamma_2 I^* + \sigma J^* - (\mu+\zeta)R^*.
\end{aligned} \tag{17}$$

Evaluation of the aforementioned system yield:

$$\begin{aligned}
S^* &= \left(\frac{(\Lambda+\zeta R^*)(\lambda^*(1-\psi)+\kappa_2)}{\mu\kappa_0 + \lambda^*((\kappa_1+\lambda^*)(1-\psi)+\kappa_2)}\right) > 0,\\
H^* &= \left(\frac{\theta(\Lambda+\zeta R^*)}{\mu\kappa_0 + \lambda^*((\kappa_1+\lambda^*)(1-\psi)+\kappa_2)}\right) > 0,\\
E^* &= \left(\frac{\lambda^*(\Lambda+\zeta R^*)((\lambda^*+\theta)(1-\psi)+\kappa_2)}{\kappa_3\mathcal{M}}\right) > 0,\\
C^* &= \left(\frac{\alpha\kappa_5(1-\tau)\lambda^*(\Lambda+\zeta R^*)((\lambda^*+\theta)(1-\psi)+\kappa_2)}{\kappa_3\{(\mu+\eta_2)\kappa_5 + \eta_1(\mu+\gamma_2+\gamma_3)\}\mathcal{M}}\right) > 0,
\end{aligned} \tag{18}$$

$$I^* = \left(\frac{\alpha\eta_1(1-\tau)\lambda^*(\Lambda+\zeta R^*)((\lambda^*+\theta)(1-\psi)+\kappa_2)}{\kappa_3\{(\mu+\eta_2)\kappa_5+\eta_1(\mu+\gamma_2+\gamma_3)\}\mathcal{M}}\right) > 0,$$
$$J^* = \left(\frac{\alpha\eta_1\gamma_3(1-\tau)\lambda^*(\Lambda+\zeta R^*)((\lambda^*+\theta)(1-\psi)+\kappa_2)}{\kappa_3\kappa_6\{(\mu+\eta_2)\kappa_5+\eta_1(\mu+\gamma_2+\gamma_3)\}\mathcal{M}}\right) > 0,$$
$$R^* = \left(\frac{\alpha\tau E^*+\eta_2 C^*+\gamma_2 I^*+\sigma J^*}{(\mu+\zeta)}\right) > 0,$$

where $\mathcal{M} = \{\mu\kappa_0+\lambda^*((\kappa_1+\lambda^*)(1-\psi)+\kappa_2)\}$.
Equation (18) can be substituted into equation (16) to produce the following polynomial with non-negative roots:

$$\Phi_2\lambda^{*2}+\Phi_1\lambda^*+\Phi_0 = 0. \tag{19}$$

Where:
$\Phi_2 = \{\alpha(1-\psi)(1-\tau)(\eta_1(\gamma_2\kappa_6+\gamma_3\sigma+\kappa_6\kappa_7)+\kappa_5\kappa_6(\eta_2+\kappa_7))+\kappa_6(1-\psi)(\alpha\tau+\kappa_7)(\kappa_5(\mu+\eta_2)+\eta_1(\mu+\gamma_2+\gamma_3))\}> 0.$
$\Phi_1 = \alpha(1-\tau)(\kappa_2+(1-\psi)\theta)\{\eta_1(\kappa_6(\gamma_2+\kappa_7)+\gamma_3\sigma)+\kappa_5\kappa_6(\eta_2+\kappa_7)\}+\kappa_6\{\kappa_5(\mu+\eta_2)+\eta_1(\mu+\gamma_2+\gamma_3)\}\{\kappa_7(\kappa_2+(1-\psi)(\kappa_3+\theta))+\alpha\tau(\kappa_2+\theta(1-\psi))\}-\alpha\beta(1-\tau)(1-\psi)\kappa_6\kappa_7(\eta_1\omega+\kappa_5).$
$\Phi_0 = \kappa_0\kappa_3\kappa_6\kappa_7(\kappa_5(\mu+\eta_2)+\eta_1(\mu+\gamma_2+\gamma_3))(1-\mathrm{R}_0).$
Since the coefficients Φ_2 and Φ_1 of λ^{*2} and λ^* are positive, it ie explicitly clear that the sign of the real roots of the polynomial equation (19) exclusively depends on the sign of Φ_0.

Theorem 5. *A distinct endemic equilibrium is exhibited by the system (1) if $\Phi_0 < 0$. This is possible iff $\mathrm{R}_0 > 1$. Consequently, the possibility of backward bifurcation for $\mathrm{R}_0 < 1$ is ruled out.*

2.7. **Global stability analysis of corruption endemic equilibrium point.** In this subsection, we demonstrate the endemic equilibrium point's global stability using the Lyapunov function as utilized by [27] . Consider the function:

$$\begin{aligned}\Pi = &\left(S-S^*+S^*\ln\frac{S^*}{S}\right)+\left(H-H^*+H^*\ln\frac{H^*}{H}\right)+\left(E-E^*+E^*\ln\frac{E^*}{E}\right)\\ &+\left(C-C^*+C^*\ln\frac{C^*}{C}\right)+\left(I-I^*+I^*\ln\frac{I^*}{I}\right)+\left(J-J^*+J^*\ln\frac{J^*}{J}\right)\\ &+\left(R-R^*+R^*\ln\frac{R^*}{R}\right).\end{aligned} \tag{20}$$

Differentiating equation (20) with respect to time gives:

$$\begin{aligned}\frac{d\Pi}{dt} = &\left(1-\frac{S^*}{S}\right)\frac{dS}{dt}+\left(1-\frac{H^*}{H}\right)\frac{dH}{dt}+\left(1-\frac{E^*}{E}\right)\frac{dE}{dt}+\left(1-\frac{C^*}{C}\right)\frac{dC}{dt}\\ &+\left(1-\frac{I^*}{I}\right)\frac{dI}{dt}+\left(1-\frac{J^*}{J}\right)\frac{dJ}{dt}+\left(1-\frac{R^*}{R}\right)\frac{dR}{dt}.\end{aligned} \tag{21}$$

After some algebraic manipulation and rearrangements, equation (21) simplifies to.

$$\begin{aligned}
\frac{d\Pi}{dt} &= \Lambda - S^*\left(\frac{\Lambda}{S} + \lambda + \kappa_1\right) + (\lambda+\kappa_1)\frac{S^{*2}}{S} + \theta S - (\lambda+\kappa_1)\frac{(S-S^*)^2}{S} - \\
& H^*\left(\frac{\theta S}{H} + (1-\psi)\lambda + \kappa_2\right) + \lambda S + (1-\psi)\lambda H + \{(1-\psi)\lambda+\kappa_2\}\frac{H^{*2}}{H} \\
& - \{(1-\psi)\lambda+\kappa_2\}\frac{(H-H^*)^2}{H} - \{S+(1-\psi)H\}\frac{E^*\lambda}{E}\kappa_3\frac{E^{*2}}{E} - \\
& \kappa_3\frac{(E-E^*)^2}{E} - \kappa_3 E^* + \alpha(1-\tau)E + \eta_1 C + \gamma_1 I - (\alpha(1-\tau)E + \gamma_1 I)\frac{C^{*2}}{C} \\
& - \kappa_4\frac{(C-C^*)^2}{L} - \kappa_4 C^* + \kappa_4\frac{C^{*2}}{C} - \eta_1 C\frac{I^*}{I} - \kappa_5\frac{(I-I^*)^2}{I} + \kappa_5\frac{I^{*2}}{I} - \\
& \kappa_5 I^* + \gamma_3 I - \gamma_3 I\frac{J^*}{J} - \kappa_6\frac{(J-J^*)^2}{J} - \kappa_6 J^* + \kappa_6\frac{{J^*}^2}{J} + \alpha\tau E + \eta_2 C + \\
& \gamma_2 I + \sigma J - \{\alpha\tau E + \eta_2 C + \gamma_2 I + \sigma J\}\frac{R^*}{R} + \kappa_7\frac{R^{*2}}{R} - \kappa_7\frac{(R-R^*)^2}{R} - \kappa_7 R^*.
\end{aligned} \tag{22}$$

Equation (22) can be expressed as $\frac{d\Pi}{dt} = \Pi_1 - \Pi_2$ where:

$$\begin{aligned}
\Pi_1 &= \Lambda + (\lambda+\kappa_1)\frac{S^{*2}}{S} + (\theta+\lambda)S + (1-\psi)\lambda H + \\
& \{(1-\psi)\lambda+\kappa_2\}\frac{H^{*2}}{H} + \kappa_3\frac{E^{*2}}{E} + \alpha E + (\eta_1+\eta_2)C + \kappa_4\frac{C^{*2}}{C} \\
& + (\gamma_1+\gamma_2+\gamma_3)I + \kappa_5\frac{I^{*2}}{I} + \sigma J + \kappa_6\frac{J^{*2}}{J} + \kappa_7\frac{R^{*2}}{R}.
\end{aligned} \tag{23}$$

$$\begin{aligned}
\Pi_2 &= \Lambda\frac{S^*}{S} + \{\lambda+\kappa_1\}S^*\left(1 + \frac{(S-S^*)^2}{SS^*}\right) + \theta S\frac{H^*}{H} + \\
& \{(1-\psi)\lambda+\kappa_2\}H^*\left(1 + \frac{(H-H^*)^2}{HH^*}\right) + \{S+(1-\psi)H\}\frac{E^*\lambda}{E} \\
& + \kappa_3 E^*\left(1 + \frac{(E-E^*)^2}{EE^*}\right) + \{\alpha(1-\tau)E + \gamma_1 I\}\frac{C^*}{C} \\
& + \kappa_4 C^*\left(1 + \frac{(C-C^*)^2}{CC^*}\right) + \eta_1 C\frac{I^*}{I} + \kappa_5 I^*\left(1 + \frac{(I-I^*)^2}{II^*}\right) \\
& + \gamma_3 I\frac{J^*}{J} + \kappa_6 J^*\left(1 + \frac{(J-J^*)^2}{JJ^*}\right) + \{\alpha\tau E + \eta_2 C + \gamma_2 I + \sigma J\}\frac{R^*}{R} \\
& + \kappa_7 R^*\left(1 + \frac{(R-R^*)^2}{RR^*}\right).
\end{aligned} \tag{24}$$

Since the model parameters are positive, we note that for $\Pi_1 < \Pi_2$, $\frac{d\Pi}{dt} < 0$. Additionally, we observe that, for $S = S^*, H = H^*, E = E^*, C = C^*, I = I^*, J = J^*$ and $R = R^*$, then, $\frac{d\Pi}{dt} = 0$. Implementation of LaSalle's Invariance Principle [21], reveals that the greatest compact invariant set in $\{(S^*, H^*, E^*, C^*, I^*, J^*, R^*) \in \Omega : \frac{d\Pi}{dt} = 0\}$ is the singleton set ε^*. Thus the endemic equilibrium ε^* is globally asymptotically stable.

Lemma 1. *The endemic equilibrium ε^* of model (1) is globally asymptotically stable whenever* $\mathrm{R}_0 > 1$.

3. Numerical Simulations

Numerical results for system (1) for various model parameter values are shown and discussed in this section. Python and Matlab are the programming languages employed in this study in the simulation process and symbolic computations. We begin by specifying the state and parameter values utilized in the developed model. The simulation results are then graphically displayed.

3.1. Parameter Estimations.

According to [22], the average life expectancy in Kenya as of September 18, 2024, was 67.70 years. The estimate of the natural death rate was calculated using the reciprocal of the life expectancy per month, which is $\frac{1}{67.70\times 12}$, as employed in [12] and [23]. We have assumed that $N_0 = 10000$ for simulation purposes, and the initial values for the state variables are $S_0 = 3550$, $H_0 = 1500$, $E_0 = 1000$, $C_0 = 500$, $I_0 = 300$, $J_0 = 200$, and $R_0 = 50$. The rate of influx Λ into a vulnerable state can be calculated using the formula $\Lambda = \mu \times N_0$. Based on estimation and the literature, the remaining parameters were identified and displayed in Table (3). Using the parameter values from Table (3), R_0 has a numerical value of $1.000942 > 1$. This implies that corruption in Kenya is bound to persist and spread if effective remedies to rebut the vice are not put in place.

Table 3. Baseline values of parameters used in the model

Parameter	Baseline value	Source
Λ	μN	To be computed
β	0.0576	Estimated
ρ	0.05	[10]
ψ	0.45	Estimated
θ	0.35	[11]
μ	1.23×10^{-3}	Computed utilising [12, 13, 24]
τ	0.20	Estimated
γ_1	0.0022	[11]
γ_2	0.015	Estimated
γ_3	0.007	Estimated
α	0.20	[25]
ζ	0.063	[26]
ω	0.80	Estimated
σ	0.125	[5]
η_1	0.040	Estimated
η_2	0.025	Estimated

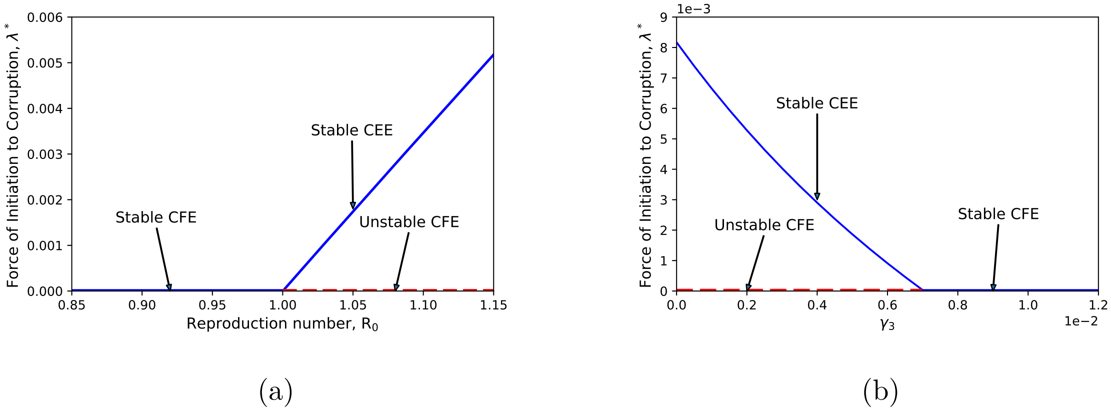

Figure 2. Graphical representation of equation (19) with the reproduction number R_0 and the incarceration rate of the corrupt persons γ_3 as the bifurcation parameters in panels (a) and (b) respectively. The branching points appear at the value of the parameter where $R_0 = 1$.

3.2. **Bifurcation diagrams.** In this subsection, we use bifurcation diagrams fig.(2) to simulate the analytical results we obtained in the preceding section. Figure 2(a), is the display of R_0 as bifurcation parameter. As R_0 rises, we observe that CFE remains stable until it reaches the branching point (BP) at $R_0 = 1$, at which time it shifts to the unstable region shown by the dotted red line. In this case, BP signals the onset of CEE, which is directly proportional to R_0. Figure 2(b) is the display of γ_3 as a bifurcation parameter. It is evident that when $\gamma_3 = 0$, we have an unstable corruption-free equilibrium (shown by the dotted red curve) and a stable endemic equilibrium (shown by the blue curve). It is clear that the force of initiation into corruption λ^* and γ_3 are inversely related. We note that at BP, the value of $\gamma_3 = 0.007039$. The endemic equilibrium vanishes after BP is passed, and CFE transforms its stability into a stable equilibrium.

3.3. **Sensitivity Analysis.** The impact of parameter values on the basic reproduction number R_0, is examined in this subsection. We assess both the impact of changing a parameter value on R_0 and the robustness of the model predictions using the estimation parameter values. If R_0 is a differentiable function with respect to each of the parameters, then the normalized forward sensitivity index of R_0 with regard to the parameter ψ is

$$\mathcal{P}_{\psi}^{\mathbf{R_0}} = \frac{\partial R_0}{\partial \psi} \times \frac{\psi}{R_0}. \tag{25}$$

The numerical values for the elasticities are now obtained using the elasticity formula provided in equation (25) with the parameter values in Table (3) and the outcomes are shown in Table (4) respectively.

Table 4. The table below shows the elasticity indices of R_0 to the model parameters evaluated at the baseline values.

Parameters	Elasticity index	Value
β	$\mathcal{P}_{\beta}^{R_0}$	+1.000000
ω	$\mathcal{P}_{\omega}^{R_0}$	+0.557200
ρ	$\mathcal{P}_{\rho}^{R_0}$	+0.080528
γ_1	$\mathcal{P}_{\gamma_1}^{R_0}$	+0.002156
ψ	$\mathcal{P}_{\psi}^{R_0}$	-0.646207
η_2	$\mathcal{P}_{\eta_2}^{R_0}$	-0.398282
γ_2	$\mathcal{P}_{\gamma_2}^{R_0}$	-0.361186
τ	$\mathcal{P}_{\tau}^{R_0}$	-0.250000
γ_3	$\mathcal{P}_{\gamma_3}^{R_0}$	-0.168553
θ	$\mathcal{P}_{\theta}^{R_0}$	-0.082509
μ	$\mathcal{P}_{\mu}^{R_0}$	-0.053344
η_1	$\mathcal{P}_{\eta_1}^{R_0}$	-0.024922

From Table (4), the parameters with positive indices suggest that a rise in value of these parameters accelerates the population's propensity for corrupt behavior, whereas the negative sensitivity indicates that an increase in the value of these parameters results in a decline in the corrupt population. We note that 10% increase in corruption initiation coefficient β correlates with 10% increase in the basic reproduction number. Conversely, 10% rise in the imprison rate of the corrupt persons γ_3 results in 1.68553% decrease in the reproduction number R_0. It is evident that the parameters with the greatest impact on corruption propagation in the community are β, ψ and ω. Figure (3) provides a concise demonstration of the global stability of the CFE state in conjunction with theorem (3). From this figure, we infer that for various initial values of the corruption-impacted compartments, all solution trajectories asymptotically converge to CFE provided that $\mathcal{R}_0 < 1$. The global stability of CEE is encapsulated in Fig.(4). The inference we derive from this figure is that for $R_0 > 1$ all solution trajectories asymptotically tend towards corruption endemic equilibrium (see lemma (1)).

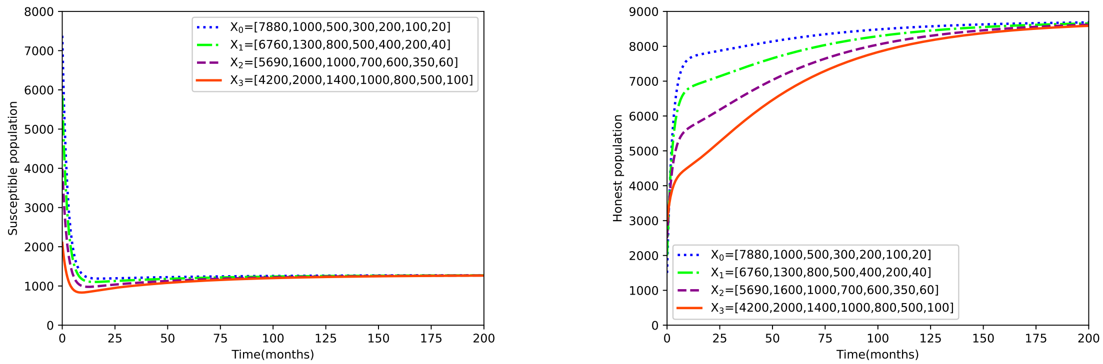

(a) (b)

FIGURE 3. The susceptible (S) and Honest (H) asymptotically approach a corruption-free equilibrium state. The parameter values utilized are those listed in Table (3) with the exception of $\beta = 0.025$, so that $\mathrm{R}_0 = 0.434437 < 1$.

Figure (5), the combined effect of varying ψ and η_1 is displayed. This result clearly shows that control measures have to be maintained at high levels for a long time in order to tame corruption. Thus, continuous anti-corruption campaigns and religious doctrine, along with the establishment of an atmosphere that supports corruption whistle blowers, adversely inhibits corruption from spreading throughout the community. Figure (6), explores the effect simultaneous implementation of three control measures i.e. ψ, η_1 and γ_3 for the exposed and the corrupt individuals. We note that public corruption is decreased when individuals found corrupt are incarcerated because it dissuades potential criminals and renders convicts incapable of initiating others to corrupt behavior. From the time series solution, we can deduce that the three-pronged approach, which entails effective anti-corruption campaign and religious teaching, increasing the rate at which corrupt individuals are identified as well of increasing the incarceration rate is the most effective strategy of immensely lowering the reproduction number and hence decreasing corruption among the citizens.

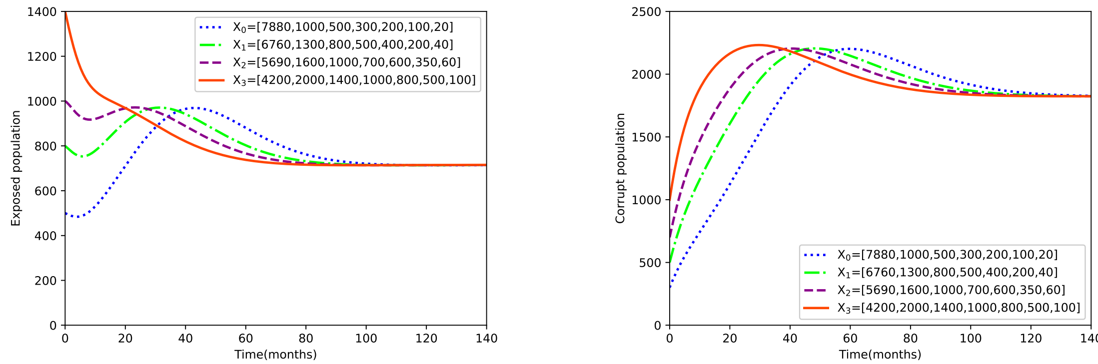

(a) (b)

FIGURE 4. The Exposed (E) and Corrupt (C) populations asymptotically approach a corruption-endemic equilibrium state. The parameter values utilized are those listed in Table (3) with the exception of $\beta = 0.240$, so that $R_0 = 4.1705920 > 1$.

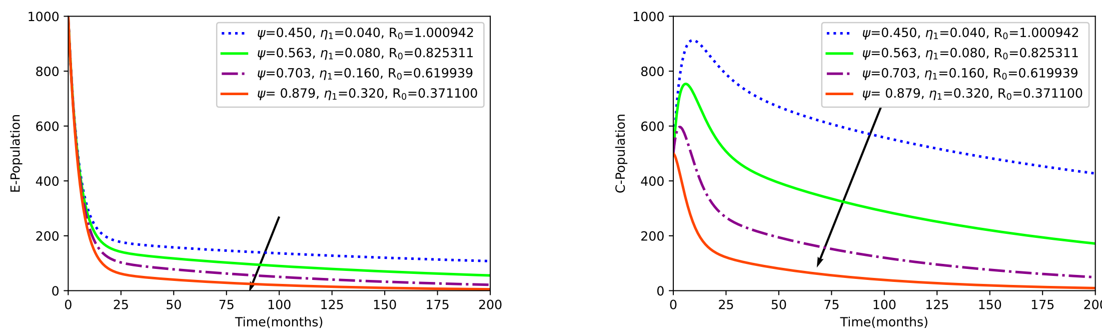

(a) (b)

FIGURE 5. Time series solution capturing the combined effects of varying the parameters ψ and η_1 for (a) Exposed population (b) Corrupt individuals, by utilizing the parameter values in Table (3)

.

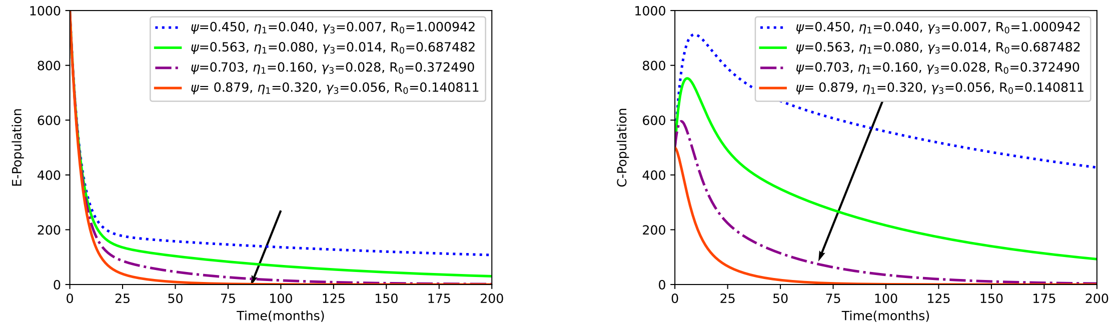

(a) (b)

Figure 6. Time series solution capturing the combined effects of varying the parameters ψ, η_1 and γ_3 for (a) Exposed population (b) Corrupt individuals, by utilizing the parameter values in Table (3)

.

4. Conclusions

In this work, a nonlinear deterministic mathematical model of corruption propagation dynamics is developed and examined. First, we determined the feasible region in which the model is found to be well-posed both mathematically and epidemiologically. The Next-Generation Matrix (NGM) approach is then used to compute the fundamental reproduction number, R_0. Routh-Hurwitz criterion and the Jacobian matrix were used to determine the CFE local stability, whereas the Castillo-Chavez and Song technique was used to evaluate the CFE global stability. The analytical solution reveals that the corruption-free equilibrium point is locally and globally asymptotically stable whenever $R_0 < 1$ and unstable whenever $R_0 > 1$. The Castillo-Chavez and Song approach was utilized to ascertain the existence and stability of the endemic equilibrium point. Using an appropriate Lyapunov function it was established that the endemic equilibrium point is globally asymptotically stable whenever $R_0 > 1$. The normalized sensitivity indices was used to determine the influence of various parameter values on R_0. It is evident that the most sensitive parameters are β and ω with positive signs. This indicates that lowering the contact rate of the susceptible and the honest populations with corrupt individuals lowers R_0 and, consequently, the corruption burden. Moreover, the parameter ψ is the most sensitive parameter with negative sign. This suggests that effective religious teachings and anti-corruption initiatives lower the contact rate which in turn reduces R_0 and so does the corruption propagation. The simulation results underscore the fact that corruption in the community is guaranteed to persist whenever $R_0 > 1$,otherwise for $R_0 < 1$, this menace would eventually fade away. Numerical simulations were conducted for the reproduction number R_0 in terms of the modification factor ω and the corruption initiation rate β. Consequently, we note from the time series solution that the reproduction number R_0 increased with the increase of these parameters. It is therefore imperative that the policymakers give priority to strategies that inhibit the initiation of vulnerable population into corrupt practices. Moreover, it can be deduced from the time series solution that the simultaneous implementation of ψ, η_1 and γ_3 causes corruption to diminish immensely. It is therefore crystal clear that in order to tame corruption a singular approach may be untenable. This study therefore proposes a three-pronged approach to combat corruption, which includes educating the public about anti-corruption issues and fostering an atmosphere that encourages moral behavior, accountability, and honesty. Second, this study emphasizes the necessity of putting in place robust whistleblowing procedures, which include removing some of the typical barriers that would prevent potential whistleblowers from disclosing any corruption-related misconduct they may encounter. Lastly, the prosecution and incarceration of the corrupt individuals irrespective of their social-economic standing if found culpable of corruption.

Competing interests: The author declares that there is no conflict of interest regarding the publication of this paper.

References

[1] A. Alesina, A. Devleeschauwer, W. Easterly, S. Kurlat, R. Wacziarg, Fractionalization, J. Econ. Growth 8 (2003), 155–194.

[2] D. Treisman, The causes of corruption: A cross-national study, J. Public Econ. 76 (2000), 399–457.

[3] N. Mkhize, S. Moyo, S. Mahoa, African solutions to African problems: A narrative of corruption in postcolonial Africa, Cogent Soc. Sci. 10 (2024), 2327133.

[4] S. Gupta, H. Davoodi, R. Alonso-Terme, Does corruption affect income inequality and poverty?, Econ. Gov. 3 (2002), 23–45.

[5] S. Abdulrahman, Stability Analysis of the Transmission Dynamics and Control of Corruption, Ph.D. thesis, 2014.

[6] O. Danford, M. Kimathi, S. Mirau, Mathematical modelling and analysis of corruption dynamics with control measures in Tanzania, J. Math. Informatics 19 (2020), 57–79.

[7] World Bank, Helping Countries Combat Corruption: The Role of the World Bank, World Bank, Washington, D.C., 1997.

[8] T.W. Gutema, A.G. Wedajo, P.R. Koya, Sensitivity and bifurcation analysis of corruption dynamics model with control measure, Int. J. Math. Ind. 16 (2024), 2450009.

[9] S.E. Adetayo, D.M. Oluwole, Impact of corruption in a society with exposed honest individuals: A mathematical model, Asia Pac. J. Math. 10 (2023), 18.

[10] B.Z. Aga, A. Geleta, T. Duressa, Corruption dynamics: A mathematical model and analysis, Front. Appl. Math. Stat. 10 (2024), 1323479.

[11] L. Lemecha, Modelling corruption dynamics and its analysis, Ethiopian J. Sci. Sustain. Dev. 5 (2019), 13–27.

[12] F.M. Muli, B. Okelo, R. Magwanga, O. Ongati, Mathematical analysis of COVID-19 model incorporating vaccination of susceptible and isolation of symptomatic individuals, J. Appl. Math. Comput. 70 (2024), 461–488.

[13] Z. Kifle, L. Obsu, Mathematical modeling for COVID-19 transmission dynamics: A case study in Ethiopia, Results Phys. 34 (2022), 105191.

[14] F.M. Muli, Mathematical analysis of drug and substance abuse model with treatment and policing, J. Appl. Math. 2025 (2025), 6666148.

[15] O. Diekmann, H. Heesterbeek, Mathematical Tools for Understanding Infectious Disease Dynamics, Princeton University Press, Princeton, 2013.

[16] O. Diekmann, J.A.P. Heesterbeek, M.G. Roberts, The construction of next-generation matrices for compartmental epidemic models, J. R. Soc. Interface 7 (2010), 873–885.

[17] L.J.S. Allen, An Introduction to Mathematical Biology, Pearson/Prentice Hall, 2017.

[18] M. Martcheva, An Introduction to Mathematical Epidemiology, Springer, New York, 2015.

[19] C. Castillo-Chavez, Z. Feng, W. Huang, P. van den Driessche, D. Kirschner, A.A. Yakubu, On the computation of R_0 and its role in global stability, Mathematical Approaches for Emerging and Re-emerging Infectious Diseases: An Introduction, Springer, New York, 2002, 31–65.

[20] C. Castillo-Chavez, B. Song, Dynamical models of tuberculosis and their applications, Math. Biosci. Eng. 1 (2004), 361–404.

[21] J.K. Hale, Ordinary Differential Equations, Robert E. Krieger Publishing Company, New York, 1981.

[22] Worldometer, Kenya population, Available online, 2024.

[23] F.B. Agusto, Optimal isolation control strategies and cost-effectiveness analysis of a two-strain avian influenza model, Math. Biosci. Eng. 113 (2013), 155–164.

[24] T.C. Sun, M.H. DarAssi, W.F. Alfwzan, M.A. Khan, A.S. Alshahrani, S.S. Alqahtani, T. Muhammad, Mathematical modeling of COVID-19 with vaccination using fractional derivative: A case study, Fractal Fract. 7 (2023), 234.

[25] Y.N. Anjam, M.I. Aslam, S.A. Cheema, S. Munawar, N. Saleem, M. Rahman, Stability analysis of the corruption dynamics under fractional-order interventions, Nonlinear Eng. 13 (2024), 20220363.

[26] T. Duressa, F. Legesse, Modelling and optimal control strategies of corruption dynamics, Appl. Math. Inf. Sci. 17 (2023), 643–654.

[27] F.M. Muli, Modeling the impact of public health education programs and relapse of the rehabilitees on drug and substance use dynamics, Int. J. Math. Ind. 18 (2026), 2650001.